J|A|C|S
ARTICLES
Published on Web 06/11/2003

Synthesis, Self-Assembly, and Switching of One-Dimensional Nanostructures from New Crowded Aromatics

Mark L. Bushey, Thuc-Quyen Nguyen, and Colin Nuckolls*

Contribution from the Department of Chemistry, Columbia University, New York, New York 10027

Received February 20, 2003; E-mail: cn37@columbia.edu

Abstract: This study outlines a versatile and expeditious synthesis of the first derivatives of a new class of benzene that is substituted with both three amide and three alkyne substituents. Sparsely covered monolayer films, made through spin-casting, reveal one-dimensional nanostructures that can be visualized with atomic force microscopy. In bulk, synchrotron X-ray diffraction and polarized light microscopy show that these nanostructured columns assemble further into a two-dimensional liquid crystalline phase. The birefringence of this phase can be switched by application of an electric field. The half-time for the liquid crystalline phase to switch is very fast and proportional to the applied voltage.

Introduction

Discotic liquid crystals[1] have a number of useful applications that are a consequence of stacking aromatic molecules in a face-to-face geometry including semiconductors,[2] ionic conductors,[3] light emitting diodes,[4] photoconductors,[5] electrooptics,[6] and nonlinear optics.[7] Our efforts,[8] as well as others',[9] are in controlling the intermolecular forces that bring the aromatic subunits together by using a combination of hydrogen bonds and π-stacking. This study describes the first experiments on a new class of hexasubstituted aromatic molecules **1** shown in Figure 1A. These structures have a central benzene ring with both amide and alkyne substituents. The three alkynes are conjugated to the central aromatic ring, meaning substituents on the alkynes can alter the reduction/oxidation potentials of the central aromatic ring and provide a path for charge injection into the stack. Shown below is a general method to synthesize these new structures and their assembly into columnar superstructures. Individual one-dimensional superstructures that are only a few nanometers wide can be visualized with atomic force microscopy (AFM). In bulk, the columns form a two-dimensional liquid crystalline phase that can be switched with the application of an electric field. The rates of this process are fast and proportional to the applied electric field strength.

(1) For leading references on discotic liquid crystals, see: (a) Guillon, D. *Struct. Bonding* **1999**, *95*, 41−82. (b) Chandrasekhar, S.; Prasad, S.; Krishna, A. *Contemp. Phys.* **1999**, *40*, 237−245. (c) Chandrasekhar, S.; Ranganath, G. S. *Rep. Prog. Phys.* **1990**, *53*, 57−84. (d) Boden, N.; Bushby, R. J.; Clements, J.; Movaghar, B. *J. Mater. Chem.* **1999**, *9*, 2081−2086. (e) *Metallomesogens*; Serrano, J. L., Ed.; VCH: New York, 1996. (f) Simon, J.; Bassoul, P. In *Phthalocyanines: Properties and Applications*; Leznoff, C. C., Lever, A. B. P., Eds.; VCH: New York, 1989; Vol. 2, Chapter 6. (g) Serrette, A. G.; Lai, C. K.; Swager, T. M. *Chem. Mater.* **1994**, *6*, 2252−68.

(2) (a) Boden, N.; Movaghar, B. *Handbook of Liquid Crystals*; Wiley-VCH: New York, 1998; Vol. 2B, pp 781−798. (b) Van de Craats, A. M.; Warman, J. M.; Fechtenkotter, A.; Brand, J. D.; Harbison, M. A.; Mullen, K. *Adv. Mater.* **1999**, *11*, 1469−1472. (c) Chandrasekhar, S.; Prasad, S. K. *Contemp. Phys.* **1999**, *40*, 237−245. (d) Boden, N.; Bushby, R. J.; Clements, J.; Movaghar, B. *J. Mater. Chem.* **1999**, *9*, 2081−2086. (e) Percec, V.; Glodde, M.; Bera, T. K.; Miura, Y.; Shiyanovskaya, I.; Singer, K. D.; Balagurusamy, V. S. K.; Heiney, P. A.; Schnell, I.; Rapp, A.; Spiess, H.-W.; Hudson, S. D.; Duan, H. *Nature* **2002,** *419*, 384−387.

(3) (a) Percec, V.; Johansson, G.; Heck, J.; Ungar, G.; Batty, S. V. *J. Chem. Soc., Perkin Trans. 1* **1993**, 1411−1420. (b) Ungar, G.; Batty, S. V.; Percec, V.; Heck, J.; Johansson, G. *Adv. Mater. Opt. Electron.* **1994**, *4*, 303−313. (c) Simon, J.; Sirlin, C. *Pure Appl. Chem.* **1989**, *61*, 1625−1629. (d) Toupance, T.; Ahsen, V.; Simon, J. *J. Chem. Soc., Chem. Commun.* **1994**, 75. (e) Sielcken, O. E.; van de Kuil, L. A.; Drenth, W.; Schoonman, J.; Nolte, R. J. M. *J. Am. Chem. Soc.* **1990**, *112*, 3086−3093.

(4) Christ, T.; Gluesen, B.; Greiner, A.; Kettner, A.; Sander, R.; Stuempflen, V.; Tsukruk, V.; Wendorff, J. H. *Adv. Mater.* **1997**, *9*, 48−52.

(5) (a) Adam, D.; Schuhmacher, P.; Simmerer, J.; Hänssling, L.; Siemensmeyer, K.; Etzbach, K. H.; Ringsdorf, H.; Haarer, D. *Nature* **1994**, *371*, 141−143. (b) Schmidt-Mende, L.; Fechtenkotter, A.; Mullen, K.; Moons, E.; Friend, R. H.; MacKenzie, J. D. *Science* **2001**, *293*, 1119−1122.

(6) (a) Scherowsky, G.; Chen, X. H. *J. Mater. Chem.* **1995**, *5*, 417−21. (b) Scherowsky, G.; Chen, X. H. *Liq. Cryst.* **1994**, *17*, 803−810. (c) Kilian, D.; Knawby, D.; Athanassopoulou, M. A.; Trzaska, S. T.; Swager, T. M.; Wrobel, S.; Haase, W. *Liq. Cryst.* **2000**, *27*, 509−521. (d) Heppke, G.; Kruerke, D.; Lohning, C.; Lotzsch, D.; Moro, D.; Muller, M.; Sawade, H. *J. Mater. Chem.* **2000**, *10*, 2657−2661. (e) Kruerke, D.; Rudquist, P.; Lagerwall, S. T.; Sawade, H.; Heppke, G. *Ferroelectrics* **2000**, *243*, 207−220. (f) Nuckolls, C.; Shao, R.; Jang, W.-G.; Clark, N. A.; Walba, D. M.; Katz, T. J. *Chem. Mater.* **2002**, *14*, 773−776. (g) Bock, H.; Helfrich, W. *Liq. Cryst.* **1992**, *12*, 697−703. (h) Bock, H.; Helfrich, W. *Liq. Cryst.* **1995**, *18*, 387−399. (i) Bock, H.; Helfrich, W. *Liq. Cryst.* **1995**, *18*, 707−713. (j) Heppke, G.; Kruerke, D.; Muller, M.; Bock, H. *Ferroelectrics* **1996**, *179*, 203−209.

(7) (a) Verbiest, T.; Van Elshocht, S.; Karuanen, M.; Hellemans, L.; Snauwaert, J.; Nuckolls, C.; Katz, T. J.; Persoons, A. *Science* **1998**, *282*, 913−915. (b) Verbiest, T.; Van Elshocht, S.; Persoons, A.; Nuckolls, C.; Phillips, K. E.; Katz, T. J. *Langmuir* **2001**, *17*, 4685−4687.

(8) (a) Bushey, M. L.; Hwang, A.; Stephens, P. W.; Nuckolls, C. *J. Am. Chem. Soc.* **2001**, *123*, 8157−8158. (b) Bushey, M. L.; Hwang, A.; Stephens, P. W.; Nuckolls, C. *Angew. Chem., Int. Ed.* **2002**, *41*, 2828−2831. (c) Nguyen, T.-Q.; Bushey, M. L.; Brus, L. E.; Nuckolls, C. *J. Am. Chem. Soc.* **2002**, *124*, 15051−15054.

(9) Hydrogen bonds used to stabilize π-stacks: (a) Matsunaga, Y.; Miyajima, N.; Nakayasu, Y.; Sakai, S.; Yonenaga, M. *Bull. Chem. Soc. Jpn.* **1988**, *61*, 207−210. (b) Brunsveld, L.; Zhang, H.; Glasbeek, M.; Vekemans, J. A. J. M.; Meijer, E. W. *J. Am. Chem. Soc.* **2000**, *122*, 6175−6182 and references therein. (c) Yasuda, Y.; Iishi, E.; Inada, H.; Shirota, Y. *Chem. Lett.* **1996**, *7*, 575−576. (d) Lightfoot, M. P.; Mair, F. S.; Pritchard, R. G.; Warren, J. E. *Chem. Commun.* **1999**, *19*, 1945−1946. (e) Ranganathan, D.; Kurur, S.; Gilardi, R.; Karle, I. L. *Biopolymers* **2000**, *54*, 289−295. (f) Paleos, C. M.; Tsiourvas, D. *Angew. Chem., Int. Ed. Engl.* **1995**, *34*, 1696−1711 and references therein. (g) Brienne, M. J.; Gabard, J.; Lehn, J. M.; Stibor, I. *J. Chem. Soc., Chem. Commun.* **1989**, *24*, 1868−70. (h) Goldmann, D.; Dietel, R.; Janietz, D.; Schmidt, C.; Wendorff, J. H. *Liq. Cryst.* **1998**, *24*, 407−411. (i) Ungar, G.; Abramic, D.; Percec, V.; Heck, J. A. *Liq. Cryst.* **1996**, *21*, 73−86. (j) Percec, V.; Ahn, C.-H.; Bera, T. K.; Ungar, G.; Yeardley, D. J. P. *Chem.-Eur. J.* **1999**, *5*, 1070−1083. (k) Malthete, J.; Levelut, A. M.; Liebert, L. *Adv. Mater.* **1992**, *4*, 37−41. (l) Pucci, D.; Veber, M.; Malthete, J. *Liq. Cryst.* **1996**, *21*, 153−155.

10.1021/ja034783a CCC: $25.00

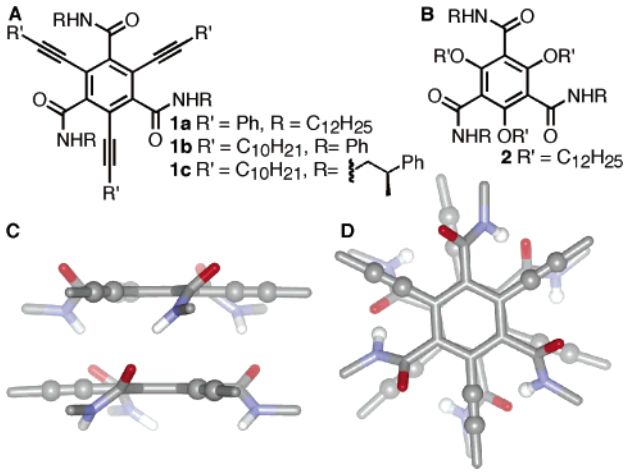

Figure 1. (a) Mesogens investigated; (b) previously studied mesogens; (c) energy minimized molecular model of **1**, side view, the modeling was performed with methyl groups on the alkynes and amides; (d) top view of the model.

Scheme 1[a]

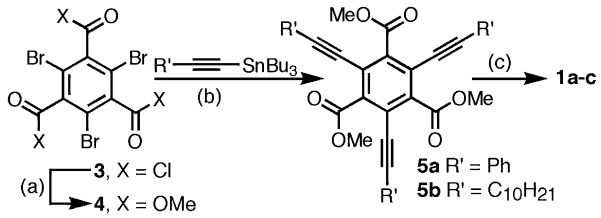

[a] Reagents and conditions: (a) MeOH, pyr, 82%; (b) $Pd(PPh_3)_4$ (cat), $AsPh_3$ (cat), 48−88%; (c) (i) KOH, *i*-PrOH; (ii) $SOCl_2$; (iii) R-NH_2, 39−66%.

The design for **1** is based on recent studies of molecules having the general structure **2**. These structures were recently shown to create very regular and stable columnar superstructures.[10] One interesting consequence of substituting the alkoxyls of **2** for the alkynes of **1** is that the six ring-substituents, by virtue of the linearity of the alkynes, cannot adopt an up/down gear-like conformation like the substituents of **2**. Shown in Figure 1c,d is an energy minimized model[11] of a dimer of **1**. This model indicates there is a synergy between hydrogen bonds and $\pi-\pi$ interactions as the central aromatic rings are stacked within their van der Waals radii (ca. 3.5 Å apart) and the amides are able to form three strong hydrogen bonds (N to O distance of ca. 2.8 Å). These models in comparison with similar ones from **2** indicate that the distance between the aromatic rings is less with alkyne substituents rather than alkoxyl substituents due to the relative size of these two groups. Moreover, the alkyne is linear and therefore should have less steric encumbrance relative to the dodecyloxy side chains.

Results and Discussion

Synthesis. Our strategy in synthesizing these molecules was to employ a palladium-mediated coupling between an alkynyl subunit and the trisbromo/triester **4**. The starting material in Scheme 1, **3**, can be made easily in 37 g batches and then converted on a multiple-gram scale into the versatile trisester **4**.[12] Unfortunately, the Sonogashira couplings[13] with **4** were sluggish and after extended reaction times gave complex mixtures from which the desired trisubstituted product could not be isolated. The key to synthesizing these molecules was employing a Farina-modified[14] Stille coupling[15] between **4** and the alkynyl stannanes.[16] Considering the demanding nature of this coupling and that the reaction is occurring three times in the same molecule, the yields of 88% for **5a** and 48% for **5b** are remarkably good. These esters can be converted to the target amides **1a**−**c** by saponification, conversion to the acid chloride, and reaction with appropriate primary amines. **1c** was synthesized as the levorotatory isomer from the enantiomerically pure (*S*)-amine. Another route that was explored to synthesize **1a**−**c** involved first the conversion of the tris-acid chloride **3** to the desired amides followed then by the palladium-mediated couplings. Although this approach also yielded **1a**−**c**, the yields for the Stille couplings were lower than those with **4**, and the desired products were extremely difficult to separate from the reaction mixture due to the polarity of the amide substituents.

AFM Imaging. By spin-casting from solution, conditions were found that produced films with monolayer thickness but sparse coverage on highly ordered pyrolytic graphite (HOPG).[17] The morphology of these films could be directly imaged with atomic force microscopy as shown in Figure 2a. For **1c**, the overwhelming feature of the micrograph is that of long and thin superstructures. The width of these structures varies over a range, with the lower limit being around one molecule wide. This dispersity in widths of the strands is indicative of the mechanism for their formation where the molecules self-associate to form isolated columns in solution which are then deposited by spin-casting.[18] Within wider samples, striations can be seen running collinear with the long axis that correlate for the diameter of an individual stack of molecules. From the height profile in Figure 2b, each feature is ca. 1.9 nm high, meaning the films are one molecule high with column axes parallel to the surface. The height of these features is ca. 3 Å higher than similar structures observed for **2**, probably due to the core of **1** being more rigid than that of **2**. These one-dimensional structures, which are only nanometers in width and microns long, are not typically seen for discotic liquid crystals.[19] These structures likely form here because the association in the stacking direction far outweighs the van der Waals forces holding the columns next to each other. Similar results were seen with **1a** and **1b**. As was seen in earlier work with **2**,[8c] the orientation of these mesogens on the surface appears to be governed by the steric encumbrance when stacking. The alkynes

(10) See ref 8 above.
(11) Molecular modeling was performed using MacroModel v. 7.0 and the Amber* forcefield: Mohamadi, F.; Richards, N. G. J.; Guida, W. C.; Liskamp, R.; Lipton, M.; Caufield, C.; Chang, G.; Hendrickson, T.; Still, W. C. *J. Comput. Chem.* **1990**, *11*, 440−467.
(12) The preparation of **3** is contained in the Supporting Information and produced by methods similar to: (a) Wallenfels, K.; Witzler, F.; Friedrich, K. *Tetrahedron* **1967**, *23*, 1845−1855. (b) Anthony, J. E.; Khan, S. I.; Rubin, Y. *Tetrahedron Lett.* **1997**, *38*, 3499−3502. (c) Hennrich, G.; Lynch, V. M.; Anslyn, E. V. *Chem.-Eur. J.* **2002**, *8*, 2274−2278.
(13) Takahashi, S.; Kuroyama, Y.; Sonogashira, K.; Hagihara, N. *Synthesis* **1980**, *8*, 627−630.
(14) Farina, V.; Krishman, B. *J. Am. Chem. Soc.* **1991**, *113*, 9585−9595.
(15) Rudisill, D. E.; Stille, J. K. *J. Org. Chem.* **1989**, *54*, 5856−5866.
(16) The preparation of tributyl(1-dodcynyl)tin is contained in the Supporting Information by a procedure similar to: Ito, Y.; Inouye, M.; Yokota, H.; Murakami, M. *J. Org. Chem.* **1990**, *55*, 2567−2568.
(17) Conditions to achieve a sparsely covered monolayer were found by varying the spin-rate, solvent, and concentration during spin-casting of **1c** on the basal plane of HOPG by the methods used in ref 8c.
(18) Nguyen, T.-Q., Bushey, M.; Martel, R.; Avouris, P.; Brus, L. E.; Nuckolls, C., unpublished results.
(19) Micron-wide crystalline domains have been seen for discotic liquid crystals: (a) Lovinger, A. J.; Nuckolls, C.; Katz, T. J. *J. Am. Chem. Soc.* **1998**, *120*, 264−268. (b) van Gorp, J. J.; Vekemans, J. A. J. M.; Meijer, E. W. *J. Am. Chem. Soc.* **2002**, *124*, 14759−14769.

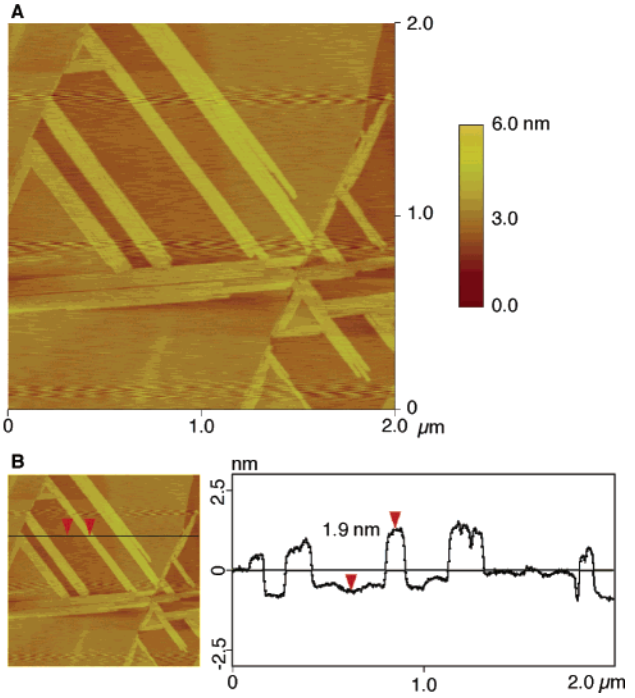

Figure 2. (a) AFM image of a sparsely covered monolayer film of **1c** on the basal plane of freshly cleaved HOPG. (b) Height profile of the film in Figure 2a.

Table 1. Phase Transition Temperatures and Enthalpies for **1a**−**c**

	heating cycle *T*/°C (Δ*H*/kJ mol^{-1})		cooling cycle *T*/°C (Δ*H*/kJ mol^{-1})	
1a	141 (9.0)	225 (dec)		
1b	96 (4.5)	225 (dec)		
1c	110 (69)	207 (15.2)	185 (−3.6)	42 (−4.7)

are sterically less demanding groups than the alkoxyls in **2** and therefore promote assembly parallel to the substrate.

Differential Scanning Calorimetry. In bulk, each of the derivatives of **1** displays similar polymorphism. The enthalpies and heats of transition for **1a**−**c** are shown in Table 1. For all three, upon heating, an initial endothermic transition is observed, indicating a transition from solid phase to a liquid crystalline phase (vide infra). The values are similar to those measured for other discotic liquid crystals.[20] For **1a** and **1b**, the transition temperature from a liquid crystalline phase to an isotropic liquid was above 225 °C where an exothermic decomposition occurred. Between the lowest endothermic transition and below the decomposition temperature, **1a** and **1b** were stable when viewed under the polarized light microscope, and the material did not show any significant discoloration. For **1c**, the transition to an isotropic liquid was at a low enough (ca. 207 °C) temperature that no exothermic decomposition occurred upon heating, and the liquid crystalline phase returned after cooling the sample. This process was stable for at least five cycles without degradation of the sample.

Polarized Light Microscopy. Shown in Figure 3 is a polarized light micrograph (at 161 °C) from a film of **1c** as it is cooled from its isotropic phase into its mesophase. It is similar to the ones formed from liquid crystalline derivatives of **2**[21] and other columnar liquid crystals,[22] particularly pyramidic

(20) For similar calorimetry values, see the references cited in ref 1.
(21) For similar micrographs from derivatives of **2**, see ref 8a,b.

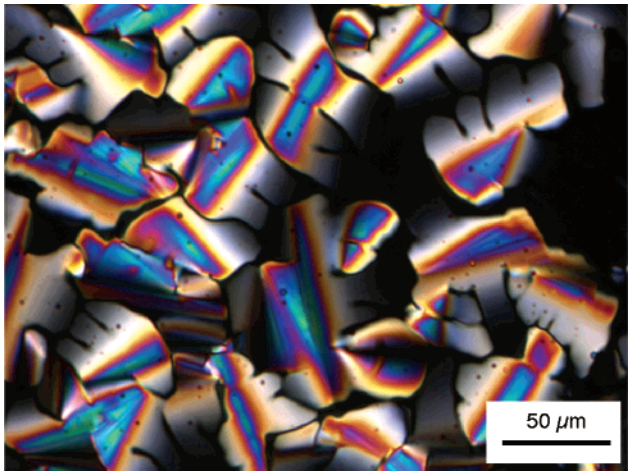

Figure 3. Polarized light micrograph for **1c** at 161 °C.

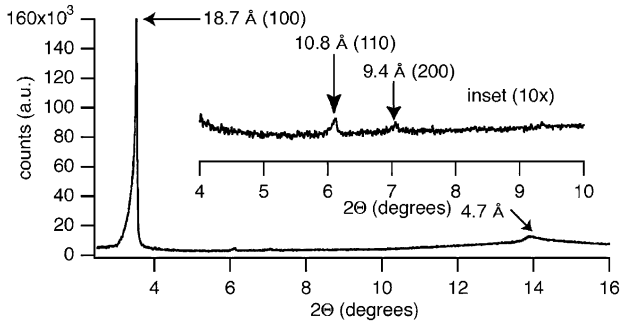

Figure 4. Synchrotron X-ray diffraction (λ = 1.15 Å) from a 2 mm Lindemann capillary tube filled with **1c** at 150 °C.

Table 2. Core-to-Core Distances for **1a**−**c** and the Columnar Arrangement

	core-to-core distances (nm)	arrangement of columns
1a	2.14	hexagonal
1b	2.02	hexagonal
1c	2.09	hexagonal

mesophases.[23] Thinner regions of these films are uniaxial and negatively birefringent, a strong indication that the mesophase is columnar in origin and that the column axes are aligned parallel to the substrate.[24]

Powder X-ray Diffraction. The synchrotron X-ray diffraction pattern for bulk samples of **1c** is shown in Figure 4. Equivalent diffraction patterns for **1a**,**b** are contained in the Supporting Information, each showing a columnar assembly whose primary reflection is between 18.1 and 19.1 Å. The core-to-core distances computed from these diffractograms are shown in Table 2. In each case, higher-order reflections allow the lattices to be indexed to a two-dimensional hexagonal arrangement of columns for **1a**−**c**. The small number of higher-order peaks in the diffractograms for **1a**−**c** and the broadness of the reflections in the alkyl region (ca. 4.5 Å) are indications that the columns are

(22) (a) Destrade, C.; Foucher, P.; Gasparoux, H.; Nguyen, H. T.; Levelut, A. M.; Malthete, J. *Mol. Cryst. Liq. Cryst.* **1984**, *106*, 121−146. (b) Billard, J.; Dubois, J. C.; Nguyen H. T.; Zann, A. *Nouv. J. Chim.* **1978**, *2*, 535−540.
(23) Zimmermann, H.; Bader, V.; Poupko, R.; Wachtel, E. J.; Luz, Z. *J. Am. Chem. Soc.* **2002**, *124*, 15286−15301.
(24) (a) Hartshorne, N. H.; Stuart, A. *Crystals and the Polarising Light Microscope*, 3rd ed.; Edward Arnold Ltd.: London, 1960; p 290ff. (b) Lovinger, A. J.; Nuckolls, C.; Katz, T. J. *J. Am. Chem. Soc.* **1998**, *120*, 264−268.

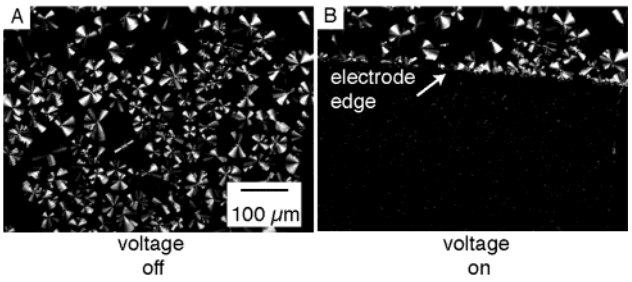

Figure 5. **1c** sandwiched between two sheets of ITO coated glass separated by 5 μm at 160 °C: (a) 0 V/μm field; (b) 20 V/μm field.

loosely correlated in a liquid crystalline phase.[25] The distances measured for **1** are similar to the 18.4−18.8 Å measured for derivatives of **2**.

Switching. Further evidence for the liquid crystallinity is seen when an electric field is applied to samples of **1c** that are sandwiched between indium tin oxide coated glass plates separated by 5 μm. A polarized light micrograph between the electrodes is displayed in Figure 5a. As compared to the samples on glass in Figure 3, the domains on ITO are much smaller. Moreover, the samples in Figure 5a are much thinner than the samples in Figure 3. Analysis of the polarization in each of the domains of Figure 5a shows that they are uniaxial and negatively birefringent (like thin regions of Figure 3), implying that these domains have their column axes parallel to the surface.[24] Some areas that are dark in Figure 5a appear bright when the sample stage is rotated, implying that the columnar axes are parallel to the polarizer or analyzer axes in the dark areas.

When an electric field is then applied to the sample, the areas that were bright now turn dark (shown in Figure 5b). This is likely due to a homeotropic alignment. This switching process is reversible, and the material shows little discoloration for many cycles at 160 °C. When the voltage across the cell is removed, the material slowly relaxes back to the parallel alignment shown in Figure 5a. Because **1a** and **1b** decompose at the temperature they became isotropic liquids, they could not be loaded into the liquid crystalline cells, and therefore the analogous experiments failed.

Shown in Figure 6a is the time that it takes for a bright, birefringent sample of **1c** (in Figure 5a) to switch to a dark state (i.e., optically isotropic, Figure 5b) at several electric field strengths. The light intensity is measured over the entire field of view. The zero time value is when the voltage is triggered across the two ITO electrodes. All of the switching processes with field strengths between 13 and 20 V/μm were complete within 1 ms. These are fast switching times for columnar liquid crystals, comparable to the fastest measured for a columnar mesophase[6c,g,h] and even faster than discotic samples that are diluted to lower their viscosity.[6f] From the curve-fit of the log-normal plot of the data in Figure 6a, it is evident that the decay is exponential. The rate of decay (from Figure 6a) of the birefringence and therefore the half-time ($\tau_{1/2}$) to go from bright to dark were calculated for each field strength. The half-times are plotted as a function of the applied electric field in Figure 6b. The data can be fit to a power function, and from this fit the power dependence is determined to be 1.04 ± 0.03.

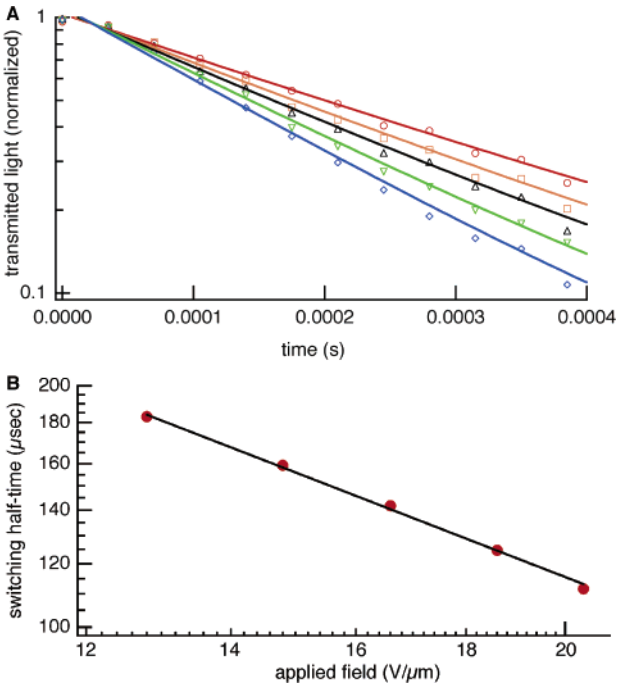

Figure 6. (a) Decrease in intensity of transmitted plane polarized light for **1c** (150 °C), as an electric field is triggered at $t = 0$ s, red = 12.8 V/μm, orange = 14.8 V/μm, black = 16.6 V/μm, green = 18.6 V/μm, blue = 20.4 V/μm; the symbols are 1/50 of the measured data, and the color-coded solid lines are the curve fit. The *y*-axis is logarithmic. (b) A plot of the half-times for switching measured from Figure 6a versus the applied electric field. The axes are logarithmic. The solid line is a power function fit to the data.

Therefore,

$$\tau_{1/2} \propto E$$

where E is the applied electric field strength, and $\tau_{1/2}$ is the half-time that characterizes the rate of the switching.

What is left unclear is whether macroscopic polarity exists in the two switching states in this system. Nematic discotics that consist of short, self-assembled columns in solution were recently shown to switch with half-times that vary as the inverse square of the applied electric field—a dielectric response.[6f] Given the difference in the power dependence, the switching mechanism in these samples is not the same as these lyotropic discotics. Possibly the packing of polar columns in **1c** cannot proceed with an all antiparallel orientation due to the inability to pack dipoles antiparallel into a hexagonal lattice.[26] Ongoing experiments are aimed at determining if this process is ferroelectric.

Conclusion

In summary, the study outlined above has shown that hexasubstituted aromatics alternatingly substituted with amides and alkynes self-assemble into columnar superstructures. In films with sparse coverage that are a monolayer in thickness, the columns can be directly visualized packing parallel to the substrate. The strands are nanometers in width and microns in length. Bulk samples display a liquid crystalline phase that can be switched with the application of an electric field. The

(25) For many examples of these characteristic diffraction patterns for columnar discotics, see: (a) Levelut, A. M. *J. Chim. Phys. Phys.-Chim. Biol.* **1983**, *80*, 149−161 and (b) the citations in ref 1.

(26) (a) Zimmermann, H.; Poupko, R.; Luz, Z.; Billard, J. *Z. Naturforsch., A* **1985**, *40A*, 149−160. (b) See also ref 1g.

switching process is fast, and its rate is proportional to the applied field strength.

Experimental Section

Atomic Force Microscopy. Solutions (between 1 mM and 1 μM) for **1** were prepared in anhydrous methylene chloride and then spun onto the basal plane of freshly cleaved HOPG substrates immediately prior to use. The films were dried in air for ~20 min before imaging. Images of the films were obtained using a Nanoscope IIIa/MultiMode Scanning Probe Microscope from Digital Instruments. Etched silicon tips with a typical spring constant of 1−5 N/m and a resonant frequency of 50−80 kHz were used. Images were collected using tapping mode and in air under ambient conditions.

Molecular Modeling. Modeling and visualization was performed on a VA Linux 420 workstation (733 MHz Intel Pentium III processor) outfitted with the Maestro Interface (Schrodinger Inc., MacroModel v. 7.0, Linux version). All models were minimized using the Amber* molecular force field.

Polarized Light Microscopy. Polarized light microscopy was performed on a Leica DMLP polarized light microscope with a 10×, 20×, or 40× objective, and an Optronics MagnaFire model S99802 digital camera system and power supply. Digital images where collected and analyzed with Image-Pro Express software version 4.0 by Media Cybernetics. Samples were placed between a cover slip and glass slide or loaded into ITO coated glass slides spaced by 5 μm (from Linkam Scientific). Photographic images were captured as the samples were cooled from their clearing temperature. The temperature was varied with a Linkam TMS 350E heating and cooling stage, with a Linkam TMS 94 heat controller and a Linkam LNP cooling system.

Switching. Experiments were performed using the microscope and camera systems described above with the addition of a Tektronix TDS 224 oscilloscope, a Tektronics CFG253 function generator, a Kepco bipolar power supply, and a Hamamatsu PMT detector. Switching experiments were performed on samples between ITO coated glass slides spaced by 5 μm that were heated in a Linkam TMS 350E heating stage equipped with electrode leads.

Synchrotron Powder X-ray Diffraction. The samples were loaded into Lindemann capillary tubes (1, 1.5, 2, and 2.5 mm). They were heated in a thermostatically controlled furnace equipped with Kapton windows. Samples were rotated 3° around the long axis of the capillary to average out any effects of preferential orientation. The X-ray diffraction measurements were performed at Beamline X3B1 of the Brookhaven National Synchrotron Light Source. X-rays of wavelength 0.702 Å and 1.151 Å, selected by a double crystal Si(111) monochromator, were incident on the sample. X-rays diffracted in the vertical plane passed through a Söller collimator of 0.03° fwhm and were detected by a conventional NaI scintillation counter. Counts were normalized to the incident flux via an ionization chamber in the incident beam.

Differential Scanning Calorimetry. DSC was performed on a Perkin-Elmer Pyris 1 Calorimeter. The samples (between 1 and 3 mg) were weighed into aluminum calorimetry pans. The pans were then sealed and analyzed. The scan rate was 20 °C/min.

General Synthetic. ^{1}H NMR (300 MHz) and ^{13}C NMR (75 MHz) spectra were recorded on a Bruker DRX 300 spectrometer. Infrared spectra were recorded on a BioRad FTS 7000 FT-IR spectrophotometer from films evaporated from solution onto a single crystal of KBr. Solvents were degassed in 20 L drums and passed through two sequential purification columns (activated alumina column followed by a supported copper catalyst column) under a positive nitrogen atmosphere.[27] Column chromatography was performed on a CombiFlash Sg100c system using RediSep normal phase silica columns (ISCO, Inc., Lincoln, NE). Tetrakis(triphenylphosphine)palladium (Strem Chemicals) and phenylethynylstannane (Aldrich) were used as received. The preparation of tributyl(1-dodcynyl)tin is contained in the Supporting Information.

2,4,6-Tribromo-1,3,5-trisbenzoyl Chloride (3). To a 1 L flask that was equipped with a reflux condenser and a stir bar were added 1,3,5-trisacetoxymethyl-2,4,6-tribromobenzyl ester[12] (37.0 g, 69.7 mmol), 3 M NaOH (175 mL, aq), $KMnO_4$ (49.6 g, 314 mmol), and H_2O (500 mL). The reaction mixture was boiled under reflux for 12 h and then cooled to room temperature. *i*-PrOH (50 mL) was added to the reaction mixture, and the solids were removed by filtration. The filter cake was washed with several portions of water, and the combined filtrate solutions were reduced in volume. The pH of the combined solutions was adjusted to ca. 1 with a concentrated HCl solution (aq). The mixture was reduced to dryness, and the flask was then equipped with a reflux condenser and a stir bar and boiled under reflux with $SOCl_2$ (200 mL) for 12 h. After being cooled to room temperature, the reaction mixture was filtered with CH_2Cl_2 washings. Distillation, under reduced pressure, yielded a white solid, **3** (30.3 g, 87%). ^{13}C NMR (75 MHz, $CDCl_3$): δ 165.4, 142.1, 115.8. IR (film KBr): 1773, 1540, 1356, 1015 cm^{-1}. HRMS (FAB) *m*/*z*: Calcd for $C_9Br_3O_3Cl_2$ $(M - Cl)^+$ 462.1936, found 462.6780.

2,4,6-Tribromobenzene-1,3,5-tricarboxylic Acid Trimethyl Ester (4). To a 200 mL flask that was equipped with a reflux condenser and a stir bar were added **3** (3.0 g, 6.00 mmol), MeOH (50 mL), and pyridine (2 mL). The reaction mixture was boiled under reflux for 12 h. After being cooled to room temperature, H_2O (50 mL) and the mixture were transferred to a separatory funnel. The two phases were separated after the addition of an HCl solution (1 M, 50 mL) and CH_2Cl_2 (100 mL). The aqueous layer was extracted with methylene chloride (3 × 100 mL), and the combined organic extracts were dried over $MgSO_4$ and concentrated under reduced pressure. Chromatography on silica gel yielded **4** as a white solid (2.41 g, 82%). ^{1}H NMR (300 MHz, $CDCl_3$): δ 3.95 (s). ^{13}C NMR (75 MHz, $CDCl_3$): δ 165.3, 138.7, 118.2, 53.9. IR (film KBr): 3010, 2960, 1730, 1550, 1460, 1440, 1370, 1350, 1240, 1180, 990 cm^{-1}. HRMS (FAB) *m*/*z*: Calcd for $C_{12}H_{10}Br_3O_6$ $(M + H)^+$ 486.8028, found 486.8026.

2,4,6-Trisphenylethynylbenzene-1,3,5-tricarboxylic Acid Trimethyl Ester (5a). An oven-dried 200 mL flask that was equipped with a reflux condenser and a stir bar was cooled under a stream of argon. Into this flask were added **4** (1.0 g, 2.05 mmol), tetrakis(triphenylphosphine)palladium (0.59 g, 5.13 mmol), triphenylarsine (0.314 g, 1.03 mmol), and tributyl(phenylethynyl)tin (2.81 g, 7.18 mmol). After the flask was evacuated and back filled with argon several times, toluene (40 mL) was added. The reaction mixture was boiled at reflux under a slight positive argon pressure for 2 days. After being cooled to room temperature, the mixture was filtered through a plug of silica gel, and combined washings were evaporated under reduced pressure. Chromatography on silica gel yielded **5a** a white solid (0.99 g, 88% yield). ^{1}H NMR (300 MHz, $CDCl_3$): δ 7.52 (m, 6H), 7.40 (m, 9H), 4.05 (s, 9H). ^{13}C NMR (75 MHz, $CDCl_3$): δ 166.8, 138.8, 132.3, 130.0, 129.0, 122.2, 121.3, 99.3, 83.3, 53.4. IR (film KBr): 3060, 3010, 2960, 2220, 1730, 1550, 1490, 1440, 1340, 1270, 1220, 1130, 1070, 1020, 960 cm^{-1}. HRMS (FAB) *m*/*z*: Calcd for $C_{36}H_{25}O_6$ $(M + H)^+$ 553.1652, found 553.1675.

2,4,6-Tri(dodec-1-ynyl)benzene-1,3,5-tricarboxylic Acid Trimethyl Ester (5b). The reaction was performed similar to that of **5a**. **4** (1.0 g, 2.05 mmol) and tributyl(1-dodcynyl)tin (3.08 g, 6.77 mmol) yielded **5b** a pale yellow oil (0.73 g, 0.99 mmol, 48%) after chromatography on silica gel. ^{1}H NMR (300 MHz, $CDCl_3$): δ 3.90 (s, 9H), 2.39 (t, J = 6.98 Hz, 6H), 1.56 (p, J = 7.2 Hz, 6H), 1.39 (m, 6H), 1.28 (m, 36H), 0.89 (t, J = 6.7 Hz, 9H). ^{13}C NMR (75 MHz, $CDCl_3$): δ 167.2, 138.8, 120.9, 100.6, 74.7, 53.0, 32.3, 30.0, 29.9, 29.7, 29.6, 29.2, 28.8, 23.1, 20.0, 14.5. IR (film KBr): 2930, 2850, 2230, 1750, 1550, 1470, 1470, 1430, 1380, 1340, 1230, 1130, 1000 cm^{-1}. HRMS (FAB) *m*/*z*: Calcd for $C_{48}H_{73}O_6$ $(M + H)^+$ 745.5408, found 745.5408.

(27) Pangborn, A. B.; Giardello, M. A.; Grubbs, R. H.; Rosen, R. K.; Timmers, F. J. *Organometallics* **1996**, *15*, 1518−1520.

2,4,6-Trisphenylethynylbenzene-1,3,5-tricarboxylic Acid, Tris-dodecylamide (1a). To a 50 mL flask that was equipped with a reflux condenser and a stir bar were added **5a** (0.29 g, 0.53 mmol), *i*-PrOH (16 mL), NaOH (2.12 g, 53.1 mmol), and H_2O (8 mL). The mixture was heated under reflux for 2 h. After the mixture was cooled to room temperature, the *i*-PrOH distilled from the reaction mixture under reduced pressure, and then acidified to ca. pH 1 with concentrated HCl. The solution was extracted with Et_2O (3 × 5 mL), and the combined organic extracts were dried over $MgSO_4$, filtered, and concentrated to dryness under reduced pressure. To this flask were then added a stir bar, reflux condenser, and $SOCl_2$ (2 mL). The reaction mixture was heated under reflux for 2 h and cooled to room temperature. After removal of the excess thionyl chloride, a viscous oil was left. To this oil were added CH_2Cl_2 (2 mL), 1-dodecylamine (0.33 g, 1.75 mmol), and pyridine (140 μL). After being stirred for 12 h, the reaction mixture was diluted with CH_2Cl_2 (5 mL) and H_2O (5 mL). The two phases were separated, and the aqueous phase was extracted with CH_2Cl_2 (3 × 10 mL). The organic extracts were combined, dried over $MgSO_4$, filtered, and concentrated to dryness. Chromatography on silica gel yielded **1a** as a waxy solid (0.34 g, 0.33 mmol, 66%). ^{1}H NMR (300 MHz, $CDCl_3$): δ 7.34−7.09 (m, 18H), 3.31 (bm, 6H), 1.48 (m, 6H), 1.3−1.1 (m, 54H), 0.91 (t, J = 6.2 Hz, 9H). ^{13}C NMR (75 MHz, $CDCl_3$): δ 166.6, 142.5, 132.3, 129.0, 128.4, 123.0, 119.4, 97.3, 84.2, 40.7, 32.4, 30.1, 30.0, 29.9, 29.8, 27.7, 23.1, 14.6. IR (film KBr): 3270, 3080, 2960, 2920, 2850, 2220, 1650, 1600, 1550, 1490, 1470, 1440, 1370, 1290, 1240, 1150, 1070, 1020 cm^{-1}. HRMS (FAB) *m*/*z*: Calcd for $C_{69}H_{93}O_3N_3$ $(M + H)^+$ 1012.7296, found 1012.7272.

2,4,6-Tri(dodec-1-ynyl)benzene-1,3,5-tricarboxylic Acid Tris-phenylamide (1b). To a 25 mL flask that was equipped with a reflux condenser and a stir bar were added **5b** (0.11 g, 0.15 mmol), *i*-PrOH (4 mL), NaOH (0.580 g, 14.5 mmol), and water (2 mL). The mixture was boiled under reflux for 12 h. After the mixture was cooled to room temperature, the *i*-PrOH distilled from the reaction mixture under reduced pressure, and then acidified to ca. pH 1 with concentrated HCl. The solution was extracted with Et_2O (3 × 5 mL), and the combined organic extracts were dried over $MgSO_4$, filtered, and concentrated to dryness under reduced pressure. To this flask were then added a stir bar, reflux condenser, and $SOCl_2$ (2 mL). The reaction mixture was heated under reflux for 2 h and cooled to room temperature. After removal of the excess thionyl chloride, a viscous oil was left. To this oil were added CH_2Cl_2 (2 mL), aniline (45 mg, 0.48 mmol, 44 μL), and pyridine (38 mg, 0.48 mmol, 40 μL). After being stirred for 12 h, the reaction mixture was diluted with CH_2Cl_2 (5 mL) and H_2O (5 mL). The two phases were separated, and the aqueous phase was extracted with CH_2Cl_2 (3 × 10 mL). The organic extracts were combined, dried over $MgSO_4$, filtered, and concentrated to dryness. Chromatography on silica gel yielded **1b** as a white, waxy solid (53 mg, 0.057 mmol, 39%). ^{1}H NMR (300 MHz, $CDCl_3$): δ 9.03 (bs, 3H), 7.76 (d, J = 7.8 Hz, 6H), 7.28 (t, J = 7.9 Hz, 6H), 7.07 (t, J = 7.2 Hz, 3H), 1.94 (t, J = 7.4 Hz, 6H), 1.15−0.91 (m, 57H). ^{13}C NMR (75 MHz, $CDCl_3$): δ 165.3, 141.1, 139.0, 129.0, 124.6, 120.9, 120.8, 101.6, 75.0, 32.4, 30.1, 29.8, 29.8, 29.5, 28.9, 23.1, 20.1, 14.6. IR (film KBr): 3290, 3250, 3190, 3140, 3080, 2960, 2920, 2850, 2230, 1660, 1600, 1550, 1500, 1440, 1320, 1260 cm^{-1}. HRMS (FAB) *m*/*z*: Calcd for $C_{63}H_{82}O_3N_3$ $(M + H)^+$ 928.6357, found 928.6328.

2,4,6-Tri(dodec-1-ynyl)benzene-1,3,5-tricarboxylic Acid Tris[(2-(*S*)-phenylpropyl)amide] (1c). **1c** was synthesized by the same procedure as **1b**. **5b** (0.10 g, 0.13 mmol) and (*S*)-2-phenyl-1-propylamine (60 mg, 0.44 mmol, 64 μL) yielded **1b** as a waxy solid (74 mg, 0.07 mmol, 52%). $[\alpha]^{23}_D = -29.5°$ (c = 1.0, CH_2Cl_2). ^{1}H NMR (300 MHz, $CDCl_3$): δ 7.33−7.23 (m, 15H), 5.58 (t, J = 6.0 Hz, 3H), 3.72 (p, J = 6.9 Hz, 3H), 3.47 (m, 3H), 3.02 (h, J = 6.9 Hz, 3H), 2.34 (t, J = 6.9 Hz, 6H), 1.54 (m, 6H), 1.35 (d, J = 6.9 Hz, 9H), 1.27 (s, 42H), 0.90 (t, J = 6.6 Hz, 9H). ^{13}C NMR (75 MHz, $CDCl_3$): δ 167.0, 144.2, 142.2, 129.2, 127.4, 127.2, 120.2, 100.0, 75.1, 47.0, 40.2, 32.3, 30.1, 30.0, 29.7, 29.4, 28.9, 23.1, 20.2, 19.4, 14.5. IR (film KBr): 3280, 3080, 3060, 3030, 2960, 2920, 2850, 2230, 1650, 1550, 1490, 1470, 1380, 1330, 1280, 1130, 1020 cm^{-1}. HRMS (FAB) *m*/*z*: Calcd for $C_{72}H_{100}O_3N_3$ $(M + H)^+$ 1054.7766, found 1054.7756.

Acknowledgment. We thank Libor Vylicky (Columbia University) for help with the electrooptic switching experiments. We acknowledge financial support from the Chemical Sciences, Geosciences and Biosciences Division, Office of Basic Energy Sciences, US D.O.E. (#DE-FG02-01ER15264) and National Science Foundation, Nanoscale Exploratory Research Grant (#DMR-01-02467). This work is supported in part by the Nanoscale Science and Engineering Initiative of the National Science Foundation under NSF Award Number CHE-0117752. This work has used the shared experimental facilities that are supported primarily by the MRSEC Program of the National Science Foundation under Award Number DMR-0213574. C.N. thanks the Beckman Young Investigator Program (2002) and the Dupont Young Investigator Program (2002) for financial support. M.L.B. thanks the ACS Division of Organic Chemistry for a graduate fellowship sponsored by Bristol-Myers Squibb. The Brookhaven National Laboratory NSLS is supported by the D.O.E., Division of Chemical Sciences and Division of Materials Sciences. The SUNY X3 Beamline at the NSLS is supported by the Division of Basic Energy Sciences of the D.O.E. (DE-FG02-86ER45231). We thank Prof. Peter Stephens (SUNY Stonybrook) for help with the powder diffraction experiments.

Supporting Information Available: Data used to characterize **1**−**5** (^{13}C NMR and ^{1}H NMR spectra). Experimental procedures for the preparation of ethynyltributylstannane and the materials for the preparation of **3**. Powder X-ray diffraction patterns for **1a** and **1b** (PDF). This material is available free of charge via the Internet at http://pubs.acs.org.

JA034783A